Fluid Phase Equilibria 370 (2014) 24–33

Contents lists available at ScienceDirect

Fluid Phase Equilibria

journal homepage: www.elsevier.com/locate/fluid

Predicting enthalpies of vaporization of aprotic ionic liquids with COSMO-RS

Bernd Schröder*, João A.P. Coutinho

CICECO, Departamento de Química, Universidade de Aveiro, Campus Universitário de Santiago, P-3810-193 Aveiro, Portugal

ARTICLE INFO

Article history:
Received 2 December 2013
Received in revised form 17 February 2014
Accepted 19 February 2014
Available online 1 March 2014

Keywords:
Aprotic ionic liquids
Enthalpies of vaporization
COSMO-RS
Hildebrand solubility parameter

ABSTRACT

Enthalpies of vaporization of a large set of ionic liquids were predicted using the COSMO-RS ion-pair approach, at $T = 298.15$ K. Comparison with currently available experimental data of different methodological origin suggests ± 10 kJ mol^{-1} as a preliminary realistic expectation range for the accuracy of COSMO-RS results. The obtained results were further used to derive the Hildebrand solubility parameters of the studied ionic liquids. While energetic subtleties due to different interaction modes in given ionic combinations are reflected in the respective enthalpies of vaporizations and are described by COSMO-RS, the presented COSMO-RS results additionally support a phenomenological data differentiation on a descriptive molecular level.

1. Introduction

For nearly a decade, the vaporization of ionic liquids was the focus of attention of a growing research community. The attraction of this subject is related to a variety of different aspects: from how to tackle the inherent experimental difficulties on a technical level, up to the understanding of the vaporization process at a molecular level, and the nature of species involved in the fluid or the vapor phase, and finally towards the question of modelling of the thermophysical parameters of vaporization. A recent review [1] provides a detailed description on the historic development of approaches, starting from the first successful thermal vaporization of aprotic ionic liquids. Ambient temperature vapour pressures of ionic liquids are very low and render the direct determination of enthalpies of vaporization a challenging task, while measurements at the high temperature end, in the range of more accessible vapour pressures, might be hampered by the onset of thermal decomposition. Due to the great difficulty of the experimental determination of enthalpies of vaporization, there is an apparent inconsistency between data sets presented by different groups. Albeit the amount of available data is constantly growing, the current situation cannot be considered as satisfactory. In response, the development of new methodologies by combining traditional techniques with recent technologies is leading the way towards more reliable data [2–4].

Accurate enthalpies of vaporizations of ionic liquids are important in the development of the theory regarding their liquid state. Vaporization equilibria data are needed in the validation of force field models applied in several simulation techniques (quantum and molecular mechanics, molecular dynamics, and Monte Carlo), as well as to anchor p–V–T parameters in equation of states and other semiempirical models.

Besides the academic interest, the enthalpy of vaporization is a thermal property of practical importance for the application of these compounds. Ionic liquids were proposed as heat-transfer fluids [5] and liquid thermal storage media in solar thermal power applications [6]. Furthermore, ionic liquids applied as electrolytes may improve the performance of dye-sensitized solar cells (DSSCs) [7]. Ionic liquids were adopted in the generation of static and stable plasma contacting with the liquid and found to be suitable for the formation of nano-composite materials using the discharge plasmas in contact with the liquids [8]. In a recent application, ionic liquid GC columns combine a wide liquidus range with the thermal stability of dicationic and polycationic bis(trifluoromethylsulfonyl)imide ionic liquids with a structure-dependent polarity differentiation, yielding columns with extended temperature ranges, while its low volatility results in lower bleed and longer column lifetimes [9].

With respect to the application of ionic liquids, the ultimate goal to achieve is generating an ionic liquid with a defined set of properties (e.g., thermal properties like the enthalpy of vaporization, or, more generally, any others physico-chemical properties) as needed by the targeted application, by concisely modifying the chemical structure of the ionic liquid on the base of structure–property

* Corresponding author. Tel.: +351 234 370200; fax: +351 234 370084.
E-mail addresses: bschroder@ua.pt, bschrode@gmx.de (B. Schröder).

http://dx.doi.org/10.1016/j.fluid.2014.02.026
0378-3812/

relations. In this sense, *in silico*-techniques are supporting synthetical efforts on an ever-increasing scale. Given additionally the constantly growing number of ionic liquids, the quest for a reliable methodology for the prediction of thermophysical properties is even more understandable [10].

Meanwhile, a wide variety of theoretical methods for the investigation of thermophysical properties exist, based on electronic structure methods, traditional molecular dynamics simulations, and first-principle molecular dynamics simulations [11]. With respect to enthalpies of vaporization, a large body of work concerning the possibility of accurately reproducing data by molecular dynamics (MD) methods is published and will not be covered here further [12–15].

In this work, we explore another theoretical approach: the estimation of enthalpies of vaporization from solvation free energies, using the COSMO-RS model. Diedenhofen et al. [16] successfully demonstrated the general capability of COSMO-RS to predict vapour pressures and enthalpies of vaporization of ionic liquids, obtaining remarkably accurate results for a small set of ionic liquids available at the time. In this paper, we extend this work to a variety of other ionic liquids, covering a broader range of cation and anion families, as well as a wider range of values of enthalpies of vaporization, evaluating the predictive capabilities of this approach at $T = 298.15$ K, for more than 100 aprotic ionic liquids.

2. Materials and methods

In COSMO-RS, the continuum solvation model for real solvents, three different ways of treating ionic liquids in mixtures were reported, depending on the chosen molecular descriptors with respect to the following assumed species [17]: (a) two ions as separate molecules with equal mole fractions, (b) the two ions merged into a meta file, and (c) (molecular) ion pair. While the latter approach, due to fixed relative orientation of anion and cation in the ion pair, does actually not describe an ionic liquid very well, it certainly reflects the physical phenomenology of ionic liquid vaporization: in 2007, Santos et al. [18] presented a first proof that the vaporization of ionic liquids occurs as a direct liquid-to-gas transfer of the ion pair. The vaporization as ion pairs was later confirmed by other techniques [19–21]. It was shown that the (molecular) ion pair approach is rather successful in the description of vapor-liquid equilibria of imidazolium based ionic liquids [16].

The ion-paired structures of all studied ionic liquids were optimized, at the BP/TZVP level of theory, both with respect to the gas phase and the COSMO state, starting from an assembled set of most probable trial structures for each ionic liquid ion pair. Prior to this step, individual ions were separately optimized and analyzed for the occurrence of possible conformers; the conformer with the lowest energy was considered for subsequent ion-pairing. DFT/COSMO (density functional theory/conductor-like screening model) calculations were performed using Turbomole V6.2 [22]. The most stable conformer for each ionic liquid was considered in the further COSMO-RS calculations. This approach corresponds to approach II as described by Diedenhofen et al. [16]. It has to be pointed out that finding the global minimum of a given ionic liquid is a time-consuming task, keeping in mind the subtle nature of the potential energy surface in each case. In fact, ionic liquids which differ only slightly in their energy and structure will yield very similar σ-profiles. In the following, the structure with the lowest energy, as found for each ionic liquid after a careful optimization procedure, is assumed to be the global minimum energy structure [23]. In order to assure to have reached a true minimum by excluding the appearance of imaginary frequencies, the encountered global gas phase minimum was subjected to vibrational frequency calculations with AOFORCE. All statistical COSMO-RS thermodynamics calculations [24] were performed with COSMOtherm Version C2.1 Revision 01. [25,26], using the parameter file BP_TZVP_C21_0110. The enthalpy of vaporization is directly obtained from theory [16].

3. Results and discussion

3.1. Experimental vs. COSMO-RS enthalpies of vaporization

A total of 102 ionic liquids formed from 41 cations and 18 anions, covering a wide range of chemical functionality, were considered in this work. A list of studied compounds, chosen abbreviations of the chemical names, as well as molar masses are given as Supplementary Data 1.

In order to obtain reliable thermophysical property data with COSMO-RS predictions, accurately optimized structures with corresponding gas-phase and COSMO state energies are necessary. Since Diedenhofen et al. [16] have successfully demonstrated that their ion-pair approach II yields, besides excellent enthalpies of vaporization data, also reasonable estimates of vapour pressures, when compared with approach I, which is based on single ions, we only consider approach II in this work. Hence, ion pairs of all ionic liquids studied here were generated and optimized. When re-optimizing already optimized gas-phase ion pairs at the BP/TZVP level in the COSMO state (ideal dielectric continuum by using COSMO with $\varepsilon_r = \infty$), a re-orientation of the ions towards themselves might occur, as previously reported [27]. This was attributed to attenuated electrostatic interactions in the continuum, as well as to reduced interionic interactions, resulting in non-uniform changes of the ion-pair structure during optimization. And another consequence arises: starting a COSMO state optimization based on the global gas-phase minimum does not necessarily lead to a global COSMO state minimum. Hence, several independent optimizations at the BP-TZVP-COSMO were performed, as well. In preliminary tests, the approach was verified based on results at $T = 298.15$ K, as published by Diedenhofen et al. [16]. Our data of enthalpies of vaporization for $[C_2C_1im][C_2SO_4]$ (164.3 kJ mol^{-1}) and $[C_4C_1im][N(CN)_2]$ (158.2 kJ mol^{-1}), calculated directly at $T = 298.15$ K, are in excellent agreement with the previously reported predictions (164.6 kJ mol^{-1} and 159.3 kJ mol^{-1}, respectively).

Table 1 is summarizing literature data of enthalpies of vaporization, at $T = 298.15$ K, for a number of ionic liquids which were determined by a variety of experimental methods. The overall agreement between the available experimental data of the same ionic liquids is of varying quality and is attributed to inherent difficulties in some of the chosen experimental approaches [28]. To evaluate COSMOtherm's performance in the prediction of enthalpies of vaporization, at $T = 298.15$ K, several experimental data were excluded from the validation set.

Results deduced from surface tension measurements [30] are deviating quite markedly for more strongly coordinating anions in the ionic liquid composition ($[PF_6]^-$ and $[BF_4]^-$). The origin of deviations in enthalpies of vaporization, as obtained with Calvet microcalorimetric experiments [18] was discussed earlier [3]. The data obtained in an earlier work by a solubility method [36], besides $[C_4C_1im][OTf]$, appear to be too high; the same holds for tunable synchrotron photoionization detection results [39] and data from TGA [34,38].

For the remaining 86 data points, an absolute relative deviation of 3.3% was calculated, corresponding to a root mean square deviation of less than 6 kJ mol^{-1} in the enthalpy of vaporization. The 86 data points are related to 41 different ionic liquids. Owed to the current situation of available data, the bulk of data points are made of alkylimidazolium based ionic liquids. In total, 15 different cations and 14 different anions occur. Two data points correspond

Table 1
Enthalpies of vaporization, $\Delta_l^g H_m^o$, at $T = 298.15$ K, as found in the literature and compared with COSMO-RS results.

Ionic liquid	$\Delta_l^g H_m^o$(COSMO-RS)/kJ mol^{-1}	Method	$\Delta_l^g H_m^o$ (Experimental)/kJ mol^{-1}	Reference
	This work	Literature		
$[C_1C_1im][NTf_2]$	130.9	QCM	128.2 ± 1.0	[28]
$[C_1C_1im][NTf_2]$	130.9	TGA	133.5 ± 1.6	[28]
$[C_2C_1im][NTf_2]$	130.1	Knudsen/QCM	133.2 ± 0.9	[3]
$[C_2C_1im][NTf_2]$	130.1	Calvet microcalorimetry	136 ± 6[a]	[18]
$[C_2C_1im][NTf_2]$	130.1	TGA	140.3 ± 2.1[b,c]	[29]
$[C_2C_1im][NTf_2]$	130.1	Knudsen	135.3 ± 1.3	[30]
$[C_2C_1im][NTf_2]$	130.1	Surface tension	136.1[a]	[30]
$[C_2C_1im][NTf_2]$	130.1	QCM	121.8 ± 1.0[c]	[31]
$[C_2C_1im][NTf_2]$	130.1	QCM	126.6 ± 1.0	[4]
$[C_2C_1im][NTf_2]$	130.1	QCM	126.9 ± 1.0	[28]
$[C_2C_1im][NTf_2]$	130.1	TGA	132.7 ± 1.5	[28]
$[C_2C_1im][NTf_2]$	130.1	Transpiration	136.7 ± 3.4	[32]
$[C_2C_1im][NTf_2]$	130.1	TPD-LOSMS	134 ± 2	[33]
$[C_2C_1im][NTf_2]$	130.1	TGA	155.5[a,c]	[34]
$[C_3C_1im][NTf_2]$	131.6	Knudsen/QCM	133.8 ± 0.5	[3]
$[C_3C_1im][NTf_2]$	131.6	QCM	129.6 ± 1.0	[28]
$[C_3C_1im][NTf_2]$	131.6	TGA	133.6 ± 2.6	[28]
$[C_3C_1im][NTf_2]$	131.6	Calvet microcalorimetry	147 ± 6[a]	[18]
$[C_4C_1im][NTf_2]$	134.3	Knudsen/QCM	139.2 ± 0.5	[3]
$[C_4C_1im][NTf_2]$	134.3	Calvet microcalorimetry	155 ± 6[a]	[18]
$[C_4C_1im][NTf_2]$	134.3	TGA	138.2 ± 0.4[b,c]	[29]
$[C_4C_1im][NTf_2]$	134.3	Knudsen	136.2 ± 1.7	[30]
$[C_4C_1im][NTf_2]$	134.3	Surface tension	134.6[a]	[30]
$[C_4C_1im][NTf_2]$	134.3	QCM	132.4 ± 2.5[c]	[35]
$[C_4C_1im][NTf_2]$	134.3	QCM	132.4 ± 1.0	[28]
$[C_4C_1im][NTf_2]$	134.3	TGA	137.8 ± 1.5	[28]
$[C_4C_1im][NTf_2]$	134.3	TPD-LOSMS	134 ± 3	[33]
$[C_4C_1im][NTf_2]$	134.3	Solubility	193[a]	[36]
$[C_4C_1im][NTf_2]$	134.3	Knudsen	138 ± 5[c]	[37]
$[C_4C_1im][NTf_2]$	134.3	TGA	154.5[a]	[38]
$[C_5C_1im][NTf_2]$	138.0	Knudsen/QCM	145.4 ± 0.5	[3]
$[C_5C_1im][NTf_2]$	138.0	QCM	136.2 ± 1.0	[28]
$[C_5C_1im][NTf_2]$	138.0	TGA	136.8 ± 1.9	[28]
$[C_5C_1im][NTf_2]$	138.0	Calvet microcalorimetry	162 ± 6[a]	[18]
$[C_6C_1im][NTf_2]$	142.7	Knudsen/QCM	150.1 ± 0.8	[3]
$[C_6C_1im][NTf_2]$	142.7	Calvet microcalorimetry	173 ± 6[a]	[18]
$[C_6C_1im][NTf_2]$	142.7	TGA	144.6 ± 0.7[b,c]	[29]
$[C_6C_1im][NTf_2]$	142.7	Knudsen	139.8 ± 0.8	[30]
$[C_6C_1im][NTf_2]$	142.7	Surface tension	141.6[a]	[30]
$[C_6C_1im][NTf_2]$	142.7	QCM	140.1 ± 2.5[c]	[35]
$[C_6C_1im][NTf_2]$	142.7	QCM	140.1 ± 1.0	[28]
$[C_6C_1im][NTf_2]$	142.7	TGA	142.3 ± 1.8	[28]
$[C_6C_1im][NTf_2]$	142.7	TPD-LOSMS	139 ± 2	[33]
$[C_7C_1im][NTf_2]$	145.7	Knudsen/QCM	153.7 ± 0.5	[3]
$[C_7C_1im][NTf_2]$	145.7	QCM	142.2 ± 1.0	[28]
$[C_7C_1im][NTf_2]$	145.7	TGA	139.9 ± 1.9	[28]
$[C_7C_1im][NTf_2]$	145.7	Calvet microcalorimetry	180 ± 6[a]	[18]
$[C_8C_1im][NTf_2]$	149.5	Knudsen/QCM	155.2 ± 0.8	[3]
$[C_8C_1im][NTf_2]$	149.5	Calvet microcalorimetry	192 ± 6[a]	[18]
$[C_8C_1im][NTf_2]$	149.5	TGA	152.8 ± 0.5[b,c]	[29]
$[C_8C_1im][NTf_2]$	149.5	Knudsen	150.0 ± 0.8	[30]
$[C_8C_1im][NTf_2]$	149.5	Surface tension	149.0[a]	[30]
$[C_8C_1im][NTf_2]$	149.5	QCM	145.7 ± 2.5[c]	[35]
$[C_8C_1im][NTf_2]$	149.5	QCM	145.7 ± 1.0	[28]
$[C_8C_1im][NTf_2]$	149.5	TGA	147 ± 1.0	[28]
$[C_8C_1im][NTf_2]$	149.5	TPD-LOSMS	149 ± 2	[33]
$[C_{10}C_1im][NTf_2]$	158.3	Knudsen/QCM	165.2 ± 0.6	[3]
$[C_{10}C_1im][NTf_2]$	158.3	TGA	155.2 ± 2.3[b,c]	[29]
$[C_{10}C_1im][NTf_2]$	158.3	Surface tension	155.5[a]	[28]
$[C_{10}C_1im][NTf_2]$	158.3	QCM	152.1 ± 2.5[c]	[35]
$[C_{10}C_1im][NTf_2]$	158.3	QCM	152.1 ± 1.0	[28]
$[C_{10}C_1im][NTf_2]$	158.3	TGA	147.5 ± 1.0	[28]
$[C_{12}C_1im][NTf_2]$	164.0	Knudsen/QCM	171.5 ± 0.8	[3]
$[C_{12}C_1im][NTf_2]$	164.0	QCM	158.0 ± 1.0	[28]
$[C_{12}C_1im][NTf_2]$	164.0	TGA	149.5 ± 1.1	[28]
$[C_{12}C_1im][NTf_2]$	164.0	QCM	158.0 ± 2.5[c]	[35]
$[C_3C_1C_1im][NTf_2]$	143.8	TGA	150.5 ± 2.2[b,c]	[29]
$[C_4C_1C_1im][NTf_2]$	147.0	Solubility	181[a]	[36]
$[C_1C_4pyrr][NTf_2]$	140.8	Tunable synchrotron photoionization detection	195 ± 19[a]	[39]
$[C_1C_4pyrr][NTf_2]$	140.8	TPD-LOSMS	152 ± 3	[40]
$[C_2C_1im][BETI]$	132.8	TGA	135.8 ± 1.8[b,c]	[29]
$[C_4C_1im][BETI]$	136.0	TGA	134.9 ± 0.4[b,c]	[29]
$[C_6C_1im][BETI]$	143.5	TGA	138.9 ± 1.6[b,c]	[29]
$[C_8C_1im][BETI]$	151.5	TGA	146.2 ± 0.8[b,c]	[29]

Table 1 (*Continued*)

Ionic liquid	$\Delta_l^g H_m^o$(COSMO-RS)/kJ mol^{-1}	Method	$\Delta_l^g H_m^o$ (Experimental)/kJ mol^{-1}	Reference
	This work	Literature		
$[C_{10}C_1im][BETI]$	160.0	TGA	148.6 ± 3.7[b,c]	[29]
$[C_3C_1C_1im][BETI]$	138.4	TGA	142.4 ± 0.5[b,c]	[29]
$[C_2C_1im][BF_4]$	145.1	QCM	135.5 ± 1.0[c]	[31]
$[C_4C_1im][BF_4]$	147.9	Surface tension	128.2[a]	[30]
$[C_4C_1im][BF_4]$	148.8	TPD-LOSMS	152 ± 2	[41]
$[C_4C_1im][BF_4]$	148.8	Solubility	203[a]	[36]
$[C_8C_1im][BF_4]$	160.7	Surface tension	122[a]	[30]
$[C_8C_1im][BF_4]$	160.7	TPD-LOSMS	162 ± 3	[33]
$[C_2C_1im][PF_6]$	144.3	QCM	143.6 ± 1.0[c]	[31]
$[C_4C_1im][PF_6]$	147.1	Solubility	191[a]	[36]
$[C_4C_1im][PF_6]$	147.1	Surface tension	154.8[a]	[30]
$[C_6C_1im][PF_6]$	152.6	Surface tension	139.8[a]	[30]
$[C_8C_1im][PF_6]$	159.4	Surface tension	144.3[a]	[30]
$[C_8C_1im][PF_6]$	159.4	TPD-LOSMS	169 ± 4	[33]
$[C_2C_1im][C_1SO_4]$	158.1	QCM	149.6 ± 1.0[c]	[31]
$[C_4py][C_1SO_4]$	172.6	TPD-LOSMS	164 ± 2	[41]
$[C_2C_1im][C_2SO_4]$	164.3	QCM	155.9 ± 1.0[c]	[31]
$[C_2C_1im][C_2SO_4]$	164.3	TPD-LOSMS	164 ± 4	[33]
$[C_4C_1im][C_8SO_4]$	189.0	TPD-LOSMS	181 ± 2	[41]
$[C_2C_1im][OTf]$	144.5	QCM	137.9 ± 1.0[c]	[31]
$[C_4C_1im][OTf]$	148.9	Solubility	141[a]	[36]
$[C_8C_1im][OTf]$	163.5	TPD-LOSMS	151 ± 3	[33]
$[C_2(C_1)_4iU][OTf]$	133.8	TPD-LOSMS	122 ± 1	[41]
$[C_2C_1im][N(CN)_2]$	155.9	Transpiration	156.4 ± 3.3	[42]
$[C_4C_1im][N(CN)_2]$	158.2	Transpiration	157.2 ± 1.1	[32]
$[C_4C_1im][N(CN)_2]$	158.2	Tunable synchrotron photoionization detection	174 ± 12 [a]	[39]
$[C_8C_1im][N(CN)_2]$	172.2	TPD-LOSMS	162 ± 4	[38]
$[C_1C_4pyrr][N(CN)_2]$	158.7	Tunable synchrotron photoionization detection	171 ± 12[a]	[39]
$[C_1C_4pyrr][N(CN)_2]$	158.7	TPD-LOSMS	161.0 ± 2.0	[43]
$[C_2C_1im][SCN]$	154.5	QCM	153.7 ± 1.0[c]	[31]
$[C_2C_1im][SCN]$	154.5	TPD-LOSMS	151 ± 2	[40]
$[C_2C_1im][PO_2(C_2H_5O)_2]$	153.4	QCM	146.1 ± 1.0[c]	[31]
$[C_2C_1im][Tos]$	172.6	QCM	166.1 ± 1.0[c]	[31]
$[C_2C_1im][PO_2(C_2F_5)_2]$	125.9	TPD-LOSMS	130 ± 2	[41]
$[C_2C_1im][FAP]$	125.6	QCM	125.8 ± 1.0[c]	[31]
$[C_6C_1im][FAP]$	137.1	TPD-LOSMS	143 ± 2	[41]
$[C_3(C_1im)_2][NTf_2]_2$	199.4	TPD-LOSMS	190 ± 15	[44]
$[C_3(C_1im)_2][NTf_2]_2$	199.4	Ion-cyclotron resonance MS	193 ± 15	[45]

Abbreviations of applied methods: QCM, quartz–crystal microbalance; TGA, thermogravimetric analysis; TPD-LOSMS, temperature-programmed desorption line-of-sight mass spectrometry.

[a] Data excluded from evaluation set.

[b] Derived from experimental data $\Delta_l^g H_m^o$ <*T*>, assuming $\Delta_l^g C_{p,m}^o = -100$ J mol^{-1} K^{-1}.

[c] Associated error assumed being identical wit the error of given $\Delta_l^g H_m^o$ <*T*>.

to the diionic $[C_3(C_1Im)_2][NTf_2]_2$. The outcome of the evaluation is depicted in Fig. 1. The overwhelming majority of data falls within a ±10 kJ mol^{-1} range. For the sake of clarity, only data sets with at least two experimentally determined data pairs are shown; available lone data pairs from Table 1 coincide to be all located well within the ±10 kJ mol^{-1} range.

Typical accuracy for enthalpies of vaporization, as obtained with COSMO-RS, is given with an order of 3 kJ mol^{-1}, but little experience for molecules of comparable molecular weight as the ionic liquids studied here was assumed [16]. From inspection of Fig. 1, ±10 kJ mol^{-1} is suggested as a preliminary realistic expectation range for the accuracy of COSMO-RS results for the molecular ion-pair approach applied in this work. Hence, the COSMO-RS approach might serve for detecting problematic experimental data which are encountered beyond this error margin.

3.2. Predicted COSMO-RS enthalpies of vaporization, liquid molar volumes, and derived Hildebrand solubility parameters of ionic liquids

COSMO-RS estimates of enthalpies of vaporization, at *T* = 298.15 K, for a wide variety of aprotic ionic liquids are given in Table 2. Besides the enthalpies of vaporization of ionic liquids composed of alkylimidazolium cations, other cations like alkylpyridinium, alkylpyrrolidinium, tetraalkylphosphonium and one example of tetraalkylammonium, were estimated, for instance, as well.

COSMOtherm was further applied to estimate a solvent's density with the integrated liquid density/volume QSPR method [46]. To validate the feasibility of the approach, densities and respective liquid molar volumes, at *T* = 298.15 K, were calculated for 62 ion pairs for which the literature data were encountered. The validation set is given as Supplementary Data 2. The absolute relative deviation amounts to 1.9% (corresponding to a root mean square deviation of 6 cm^3 mol^{-1}). Hence, all liquid molar volumes were calculated following this method, with the results given in Table 2.

From these data, Hildebrand solubility parameters of all ionic liquids studied were derived according to Eq. (1), at *T* = 298.15 K, and are given as additional information in Table 2:

$$\delta = \left(\frac{\Delta_l^g H_m^o - RT}{V_m} \right)^{1/2} \quad (1)$$

with $\Delta_l^g H_m^o$ – enthalpy of vaporization, *R* – universal gas constant, *T* – temperature and V_m – liquid molar volume.

The Hildebrand solubility parameter finds application in the prediction of solvency of solvents towards non-electrolyte solutes;

Table 2
Predicted COSMO-RS enthalpies of vaporization, $\Delta_l^g H_m^o$ (COSMO-RS), liquid molar volumes, V_m, as well as derived Hildebrand parameter, δ, and cohesive pressures, c, at $T = 298.15$ K.

No.	Ionic liquid	$\Delta_l^g H_m^o$ (COSMO-RS)/kJ mol^{-1}	V_m/(cm^3 mol^{-1})	δ/MPa$^{(1/2)}$	c/MPa
1	[C_2C_1im][NTf_2]	130.1	262.0	22.1	487.1
2	[C_3C_1im][NTf_2]	131.6	280.4	21.5	460.4
3	[C_4C_1im][NTf_2]	134.3	295.9	21.1	445.5
4	[C_5C_1im][NTf_2]	138.0	312.6	20.8	433.4
5	[C_6C_1im][NTf_2]	142.7	331.1	20.6	423.4
6	[C_7C_1im][NTf_2]	145.7	347.1	20.3	412.5
7	[C_8C_1im][NTf_2]	149.5	363.1	20.1	404.8
8	[C_9C_1im][NTf_2]	153.0	379.6	19.9	396.6
9	[$C_{10}C_1$im][NTf_2]	158.3	397.4	19.8	392.2
10	[$C_{12}C_1$im][NTf_2]	164.0	432.8	19.3	373.3
11	[C_1C_1im][NTf_2]	130.9	245.5	22.9	523.2
12	[C_2C_2im][NTf_2]	130.4	282.1	21.3	453.5
13	[C_3C_3im][NTf_2]	133.1	317.2	20.3	411.9
14	[C_4C_4im][NTf_2]	139.4	348.9	19.8	392.5
15	[C_5C_5im][NTf_2]	145.9	380.2	19.4	377.2
16	[C_6C_6im][NTf_2]	154.1	413.7	19.1	366.6
17	[C_2C_3im][NTf_2]	131.3	298.0	20.8	432.2
18	[$C_2C_1C_1$im][NTf_2]	141.6	277.7	22.4	501.0
19	[$C_3C_1C_1$im][NTf_2]	143.8	295.5	21.9	478.3
20	[$C_4C_1C_1$im][NTf_2]	147.0	312.0	21.5	463.1
21	[C_1C_2pyrr][NTf_2]	138.0	277.3	22.1	488.6
22	[C_1C_3pyrr][NTf_2]	138.5	292.1	21.6	465.8
23	[C_1C_4pyrr][NTf_2]	140.8	308.5	21.2	448.2
24	[C_1C_2pip][NTf_2]	139.6	288.1	21.8	476.0
25	[C_1C_3pip][NTf_2]	138.7	304.2	21.2	447.9
26	[C_1C_4pip][NTf_2]	140.1	318.4	20.8	432.3
27	[C_1C_2morph][NTf_2]	152.1	278.2	23.2	537.8
28	[C_1C_3morph][NTf_2]	151.7	296.6	22.4	503.2
29	[C_1C_4morph][NTf_2]	153.5	314.5	21.9	480.2
30	[C_2py][NTf_2]	143.9	258.9	23.4	546.1
31	[C_3py][NTf_2]	143.1	273.7	22.7	513.5
32	[C_4py][NTf_2]	145.8	290.0	22.2	494.2
33	[C_2-2-C_2py][NTf_2]	143.2	290.1	22.0	485.0
34	[C_3-3-C_1py][NTf_2]	138.6	293.2	21.5	464.4
35	[C_3-4-C_1py][NTf_2]	143.4	291.5	22.0	483.4
36	[N_{8881}][NTf_2]	191.1	591.3	17.9	319.0
37	[P_{8881}][NTf_2]	192.3	601.7	17.8	315.4
38	[P_{66614}][NTf_2]	219.0	713.6	17.4	303.4
39	[C_2C_1im][BETI]	132.8	318.8	20.2	408.9
40	[C_3C_1im][BETI]	133.4	334.6	19.8	391.3
41	[C_4C_1im][BETI]	136.0	349.5	19.5	382.1
42	[C_6C_1im][BETI]	143.5	382.8	19.2	368.3
43	[C_8C_1im][BETI]	151.5	415.8	18.9	358.5
44	[$C_{10}C_1$im][BETI]	160.0	451.4	18.7	348.8
45	[$C_3C_1C_1$im][BETI]	138.4	353.1	19.6	385.0
46	[C2C1im][NF_2]	139.8	203.1	26.0	676.2
47	[C_4C_1im][NF_2]	143.3	238.2	24.3	591.3
48	[C_6C_1im][NF_2]	149.5	271.4	23.3	541.6
49	[C_2C_1im][BF_4]	145.1	158.8	30.0	898.0
50	[C_4C_1im][BF_4]	148.8	193.3	27.5	756.8
51	[C_6C_1im][BF_4]	155.6	226.8	26.0	675.2
52	[C_8C_1im][BF_4]	160.7	259.8	24.7	609.1
53	[$C_2C_1C_1$im][BF_4]	148.6	176.0	28.8	830.2
54	[$C_4C_1C_1$im][BF_4]	153.7	210.7	26.8	717.6
55	[C_4-4-C_1py][BF_4]	158.7	205.9	27.5	758.8
56	[C_2C_1im][PF_6]	144.3	181.1	28.0	783.1
57	[C_4C_1im][PF_6]	147.1	216.9	25.8	666.7
58	[C_6C_1im][PF_6]	152.6	250.2	24.5	599.9
59	[C_8C_1im][PF_6]	159.4	288.1	23.3	544.5
60	[$C_4C_1C_1$im][PF_6]	154.3	232.4	25.6	653.2
61	[C_1C_1im][C_1SO_4]	161.7	158.0	31.7	1007.5
62	[C_2C_1im][C_1SO_4]	158.1	175.6	29.8	886.2
63	[C_3C_1im][C_1SO_4]	158.9	192.2	28.5	813.7
64	[C_4C_1im][C_1SO_4]	162.3	208.6	27.7	766.0
65	[C_6C_1im][C_1SO_4]	169.0	242.5	26.2	686.8
66	[C_4py][C_1SO_4]	172.6	205.7	28.8	827.2
67	[C_2C_1im][C_2SO_4]	164.3	193.0	29.0	838.8
68	[C_3C_1im][C_2SO_4]	163.6	209.0	27.8	770.8
69	[C_2py][C_2SO_4]	173.1	185.9	30.3	917.8
70	[C_2-3-C_1py][C_2SO_4]	166.1	202.8	28.4	806.8
71	[C_2C_1im][C_8SO_4]	185.0	293.4	24.9	622.1
72	[C_4C_1im][C_8SO_4]	189.0	326.6	23.9	571.1
73	[C_2C_1im][C_1SO_3]	149.1	166.7	29.7	879.5
74	[C_4C_1im][C_1SO_3]	153.9	199.6	27.5	758.4
75	[C_6C_1im][C_1SO_3]	161.6	232.9	26.1	683.3

Table 2 (*Continued*)

No.	Ionic liquid	$\Delta_l^g H_m^o$ (COSMO-RS)/kJ mol^{-1}	V_m/(cm^3 mol^{-1})	δ/MPa$^{(1/2)}$	c/MPa
76	$[C_8C_1im][C_1SO_3]$	169.7	266.3	25.1	628.0
77	$[C_2C_1im][OTf]$	144.5	188.7	27.4	752.7
78	$[C_4C_1im][OTf]$	148.9	223.0	25.6	656.8
79	$[C_6C_1im][OTf]$	155.5	255.7	24.5	598.5
80	$[C_8C_1im][OTf]$	163.5	290.1	23.6	555.0
81	$[C_2(C_1)_4iU][OTf]$	133.8	236.8	23.5	554.5
82	$[C_2C_1im][N(CN)_2]$	155.9	166.2	30.4	923.7
83	$[C_4C_1im][N(CN)_2]$	158.2	200.1	27.9	778.4
84	$[C_6C_1im][N(CN)_2]$	165.0	233.6	26.4	695.4
85	$[C_8C_1im][N(CN)_2]$	172.2	267.1	25.2	635.7
86	$[C_1C_2pyrr][N(CN)_2]$	154.0	176.9	29.3	856.6
87	$[C_1C_3pyrr][N(CN)_2]$	156.7	192.7	28.3	800.5
88	$[C_1C_4pyrr][N(CN)_2]$	158.7	210.6	27.2	742.1
89	$[C_2C_1im][SCN]$	154.5	151.1	31.7	1006.1
90	$[C_4C_1im][SCN]$	158.7	186.7	28.9	836.9
91	$[C_6C_1im][SCN]$	168.0	218.3	27.5	758.3
92	$[C_2C_1im][FAP]$	125.6	342.3	19.0	360.6
93	$[C_4C_1im][FAP]$	129.5	376.8	18.4	337.1
94	$[C_6C_1im][FAP]$	137.1	406.9	18.2	330.9
95	$[C_2C_1im][BTTI]$	145.1	423.0	18.4	337.1
96	$[C_4C_1im][BTTI]$	147.6	455.5	17.9	318.6
97	$[C_6C_1im][BTTI]$	155.2	486.5	17.7	313.9
98	$[C_2C_1im][Tos]$	172.6	233.4	27.0	728.9
99	$[C_2C_1im][PO_2(C_2F_5)_2]$	125.9	278.1	21.1	443.7
100	$[C_4C_1im][ClO_4]$	150.6	193.5	27.7	765.8
101	$[C_4C_1im][TFSM]$	151.2	364.7	20.2	407.7
102	$[C_3(C_1im)_2][NTf_2]_2$	199.4	489.0	20.1	402.7

solvents are expected to be miscible if δ is not differing by more than 3 units. This threshold value lies well above the estimated error margin of the presented data (estimated with $\Delta\delta < 0.6$ MPa$^{1/2}$). The applicability of the concept of Hildebrand solubility parameters to ionic liquids solubility was recently discussed [47]. Furthermore, Hildebrand solubility parameters contain qualitative information about the respective ionic liquids on a molecular level. The term inside the brackets is the cohesive pressure c, a measure of the total molecular cohesion per unit volume, representing the total strength of all intermolecular solvent–solvent interactions. Cohesive pressure is related to the energy required in cavity formation in a liquid [48]. In general terms, the Hildebrand solubility parameter (a cohesion parameter, as coined by Barton [49]) is a measure of the strength of molecular interactions occurring between solvent molecules. When compared with common molecular organic solvents, the ionic liquids studied in this work cover a wide polarity range, from non-polar solvents similar to tetrachloromethane ($\delta = 17.6$ MPa$^{1/2}$) [49] (ionic liquids with long alkyl chains and/or heavily fluorinated anions $[P_{66614}][NTf_2]$, $[C_6C_1im][BTTI]$) towards polar molecules even beyond ethane-1,2-diol ($\delta = 29.9$ MPa$^{1/2}$) [49] (ionic liquids with short alkyl chains and highly polar anions, like $[C_2C_1im][N(CN)_2]$, $[C_2C_1im][SCN]$ and $[C_1C_1im][C_1SO_4]$).

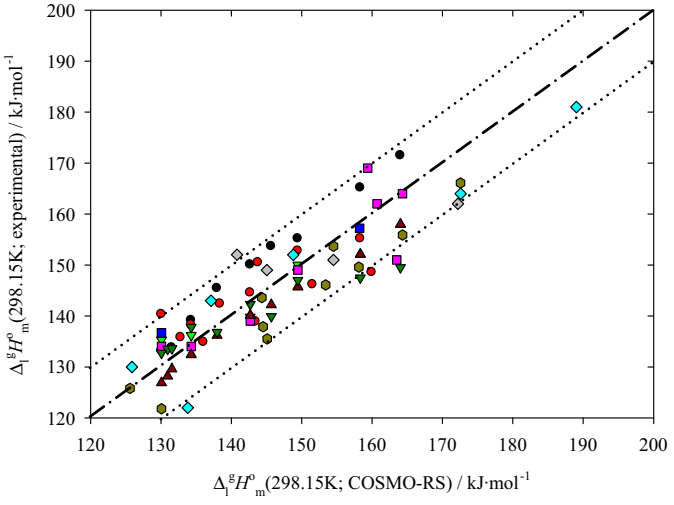

Fig. 1. Plot of the validation results of experimental enthalpies of vaporization versus the COSMO-RS results, at $T = 298.15$ K, with data arranged in an order of available experimental sets, obtained with different methodologies. ● : QCM/Knudsen – Rocha et al. 2011 [3]; ● : TGA – Luo et al. 2008 [29]; ▼ : Knudsen – Zaitsau et al. 2006 [30]; ▲ : QCM – Zaitsau et al. 2011 [35]; ■ : transpiration – Emel'yanenko et al. 2007 [32]; ■ : TPD-LOSMS – Armstrong et al. 2007 [33]; ◆ : TPD-LOSMS – Deyko et al. 2012 [41]; ◆ : TPD-LOSMS – Deyko et al. 2009 [40]; ▲ : QCM – Verevkin et al. 2013 [28]; ▼ : TGA – Verevkin et al. 2013 [28]; ⬢ : QCM – Zaitsau et al. 2012 [31].

The complexity of ionic liquids, combined with the current inconsistency of existing data sets on enthalpies of vaporization, impedes assumptions or correlations usually applied to molecular fluids [1]. Nevertheless, an appreciable amount of work was dedicated in establishing structure–property relations to all kinds of physico-chemical properties of ionic liquids [10]. More recently, with respect to enthalpies of vaporization, Zaitsau et al. [31] published a study on the influence of various anions in 1-ethyl-3-methylimidazolium based ionic liquids, taking into consideration static dielectric constants, solvent polarities, anion polarizabilities, densities, molar volumes, molar mass, surface tension, parachor, ^{1}H NMR shifts and maxima of low-frequency vibrational bands as obtained from FTIR experiments, proposing a group-contribution scheme for alkylimidazolium ionic liquids. Deyko et al. [41] proposed a scheme based on the liquid molar volume, while decomposing the enthalpy of vaporization into a Coulombic component and cationic and anionic van der Waals components. While offering the capability to calculate enthalpies of vaporization from just the chemical formula of the ionic liquid, the limits of this approach are pointed out when reaching shorter alkyl chain lengths or with other functional groups involved. In this work, we are mainly focused on the relation that can be established between enthalpies of vaporization and the liquid molar volume.

3.3. Chain-length impact of alkylimidazolium based ionic liquids

Nearly constant incremental increase of the enthalpies of vaporization with the liquid molar volume is only reached starting with

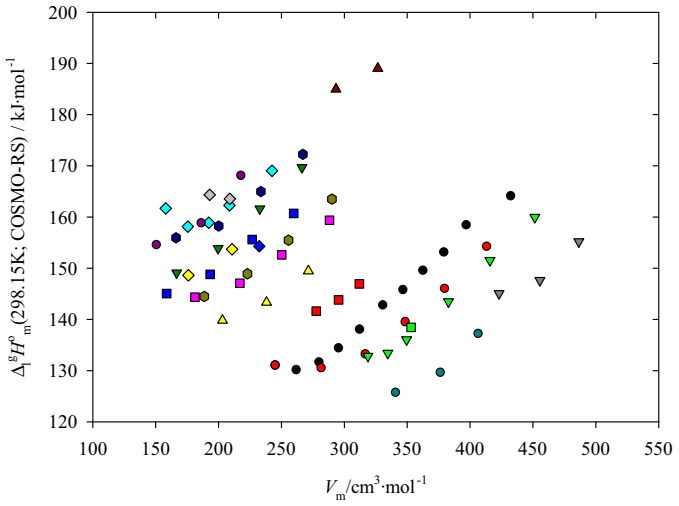

Fig. 2. Enthalpies of vaporization of alkylimidazolium based ionic liquids, at T = 298.15 K, as obtained with COSMO-RS, plotted against the respective liquid molar volume. ●: $[C_xC_1im][NTf_2]$; ●: $[C_xC_xim][NTf_2]$; ▼: $[C_xC_1im][BETI]$; ▲: $[C_xC_1im][NF_2]$; ■: $[C_xC_1im][BF_4]$; ■: $[C_xC_1im][PF_6]$; ◆: $[C_xC_1im][C_1SO_4]$; ◆: $[C_xC_1im][C_2SO_4]$; ▲: $[C_xC_1im][C_8SO_4]$; ▼: $[C_xC_1im][C_1SO_3]$; ⬢: $[C_xC_1im][OTf]$; ⬢: [CxC1im][N(CN)2]; ●: $[C_xC_1im][SCN]$; ●: $[C_xC_1im][FAP]$; ▼: $[C_xC_1im][BTTI]$; ■: $[C_xC_1C_1im][NTf_2]$; ■: $[C_3C_1C_1im][BETI]$; ◆: $[C_xC_1C_1im][BF_4]$; ◆: $[C_4C_1C_1im][PF_6]$.

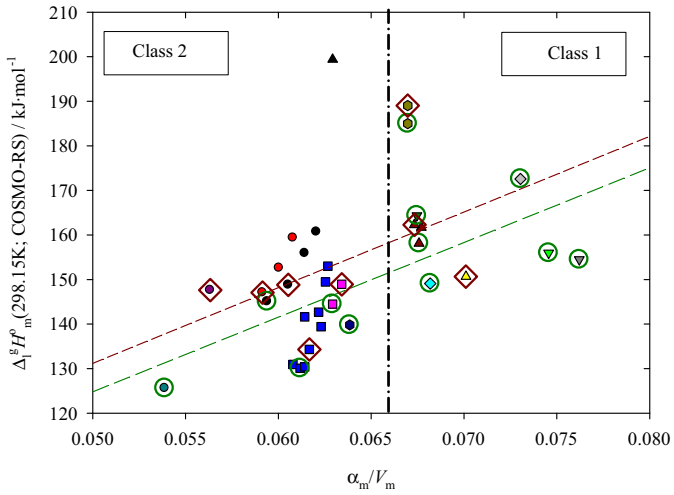

Fig. 3. Predicted enthalpies of vaporization plotted against the molar volumic polarizability, at T = 298.15 K. ●: $[C_xC_1im][BF_4]$; ●: $[C_xC_1im][PF_6]$; ▼: $[C_2C_1im][N(CN)_2]$; ▲: $[C_4C_1im][ClO_4]$; ■: $[C_xC_yC_zim][NTf_2]$; ■: $[C_xC_1im][OTf]$; ◆: $[C_2C_1im][C_1SO_3]$; ◆: $[C_2C_1im][Tos]$; ▲: $[C_xC_1im][C_1SO_4]$; ▼: $[C_2C_1im][C_2SO_4]$; ⬢: $[C_xC_1im][C_8SO_4]$; ⬢: $[C_2C_1im][NF_2]$; ●: $[C_4C_1im][BTTI]$; ●: $[C_2C_1im][FAP]$; ▼: $[C_2C_1im][SCN]$; ▲: $[C_3(C_1im)_2][NTf_2]_2$ [a]; ○: symbols inside dark-green circles: Ils with $[C_2C_1im]^+$-cations; ◇: symbols inside dark-red diamonds: Ils with $[C_4C_1im]^+$-cations. [a] – molar volumic polarizability at T = 296.15 K.

the respective ion combination with $[C_3C_1im]^+$. COSMO-RS-results for $[C_1C_1im]^+$ and $[C_2C_1im]^+$ reproduce the different incremental behaviour as found by experiment, e.g., [3], with enthalpies of vaporization higher than expected from regression of the remaining homologous series, as presented in Fig. 2, indicating the increasing importance of interactions other than dispersive ones in ionic liquids made of the smallest cations in the alkylimidazolium series. Nano-structural effects on the enthalpies of vaporization have been reported from experiment [3,50–53] and suggested by molecular dynamics simulation [54–56], and disputed by some other authors [28]. These effects are not observable with COSMO-RS. A successive elongation of the alkyl chain results in a nearly constant and roughly similar slope for all ionic liquids, indicating no significant change in the electrostatic interactions. In the case of alkylimidazolium alkylsulfate ionic iquids, the introduction of methylene groups has a comparable enthalpic effect, independent of its insertion in the alkyl chain of the alkylimidazolium or alkylsulfate moieties (e.g., the enthalpies of vaporization of $[C_4C_1im][C_1SO_4]$ and $[C_3C_1im][C_2SO_4]$ are predicted to be very similar).

Inspecting the plot, information about the difference in magnitude of the intermolecular interactions between the series can be readily extracted. From the figure, it may further be concluded that alkylimidazolium ionic liquids with an additional methyl group in the 2-position are forming separate series. To the best of our knowledge, besides the thermogravimetric data on enthalpies of vaporization of $[C_3C_1C_1im][NTf_2]$ and $[C_3C_1C_1im][BETI]$ published by Luo et al. [29], no further experimental data for any ion combination for this type of alky imidazolium based ionic liquids are currently available. The introduction of a methyl group in the 2-position will have a destabilizing effect on the hydrogen-bond network and will lead to changes on a structural level and in physicochemical properties. It was shown earlier that despite expectations, C2-methylated ionic liquids have higher melting points and viscosities than their C2-protonated counterparts [57,58]. Ludwig et al. [59,60] hypothesized that ions in C2-methylated ionic liquids form a Coulombic network and stabilize the whole system, whereas in the C2-protonated ionic liquids, the formation of H-bonds between the anion and the H–C2 of the imidazolium ring weakens the Coulombic network, hence destabilizing the system and resulting in lower melting points and viscosities, which also might explain the differences in the enthalpies of vaporization between methylated and protonated species, besides the incremental increase following the introduction of a methyl group.

In order to gain further insight into the molecular forces governing the enthalpy of vaporization of a given ionic liquid, other correlations might be applied; e.g., Shimizu et al. [61] reported on the relation between refractive indices and cohesive internal energies. In a recent comprehensive analysis of refractive index and density data of alkylimidazolium-based ionic liquids, Bica et al. [62] found that refractive indices might increase or decrease with increasing 1-alkyl chain length, depending on the nature of the anion. They emphasized different trends between Class 1 ionic liquids (ionic liquids with highly polar anions will lead to decreasing refractive indices) and Class 2 ionic liquids (ionic liquids with a large number of fluorine atoms, possessing relatively low polarizabilities and large effective atomic volumes will result in increasing refractive indices). Both classes converge with increasing 1-alkyl chain length towards a refractive index of 1.446, corresponding to a ratio of α_m/V_m of 0.0661 (or α_{CH2}/V_{CH2}). Plotting the enthalpies of vaporization against this ratio, considering the learning data set of refractive indices and densities of Bica et al. [62] for alkylimidazolium ionic liquids calculated in this work, plus additional experimental data covering a wider range of ionic liquids on the anion side, namely $[C_2C_1im][NF_2]$, $[C_4C_1im][BTTI]$, $[C_2C_1im][FAP]$, $[C_2C_1im][SCN]$ (all data from [63]), and the diionic $[C_3(C_1im)_2][NTf_2]_2$ (both density and refractive index measured in this case at T = 296.15 K [64]), Fig. 3 is obtained.

Furthermore, ionic liquids containing 1-ethylimidazolium and 1-butylimidazolium cations are separately marked. No useful correlation can be extracted from the plot – with polarizability as a measure of the strength of dispersive interactions, other interaction contributions to the enthalpy of vaporization are missing. The distance between both regression lines represents the incremental change in enthalpies of vaporization connected to the elongation of the alkyl side chain.

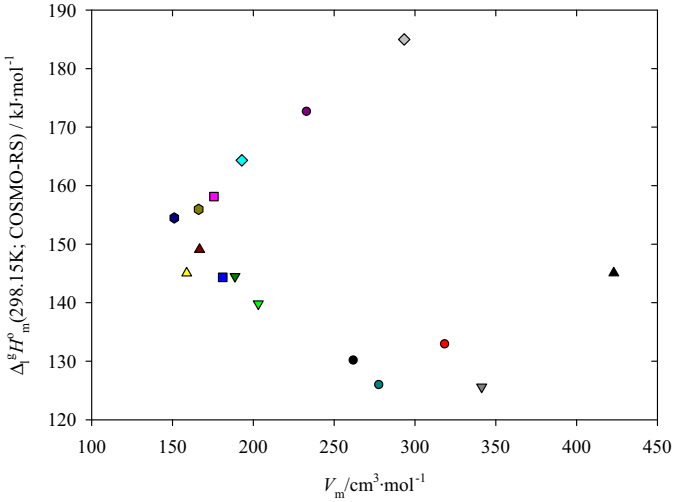

Fig. 4. Predicted enthalpies of vaporization of 1-ethyl-3-methylimidazolium based ionic liquids, at T = 298.15 K, as obtained with COSMO-RS, plotted against their respective liquid molar volume. ● : [C_2mim][NTf_2]; ● : [C_2mim][BETI]; ▼ : [C_2mim][NF_2]; ▲ : [C_2mim][BF_4]; ■ : [C_2mim][PF_6]; ■ : [C_2mim][C_1SO_4]; ◆ : [C_2mim][C_2SO_4]; ◆ : [C_2mim][C_8SO_4]; ▲ : [C_2mim][C_1SO_3]; ▼ : [C_2mim][OTf]; ⬢ : [C_2C_1im][$N(CN)_2$]; ⬢ : [C_2C_1im][SCN]; ● : [C_2C_1im][Tos]; ● : [C_2C_1im][$PO_2(C_2F_5)_2$]; ▼ : [C_2C_1im][FAP]; ▲ : [C_2C_1im][BTTI].

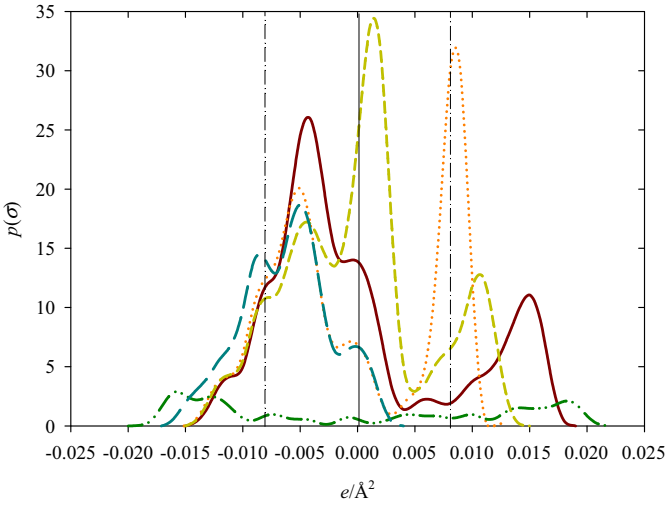

Fig. 5. Sigma profile examples of ion pairs with 1-ethyl-3-methylimidazolium cations. Sigma profiles of water and 1-ethyl-3-methylimidazolium cation are given as reference. (Brown) solid line – [C_2C_1im][C_2SO_4]; (olive-green) dashed line – [C_2C_1im][NTf_2]; (orange) dotted line – [C_2C_1im][PF_6]; (purple) short dash-dotted line – [C_2C_1im$^+$]; (turquoise) dashed line – H_2O; (grey) vertical dash-dotted lines – cut-off values for hydrogen bond donors ($\sigma_{HB} < -0.0082\,e$/Å^2) and hydrogen bond acceptors ($\sigma_{HB} > +0.0082\,e$/Å^2); (grey) vertical solid line – $\pm 0\,e$/Å^2. (For interpretation of the references to color in text, the reader is referred to the web version of this article.)

3.4. Same cation, different anions

The presence of two distinct ionic liquid classes is further noticed from inspection of the plot of COSMO-RS enthalpies of vaporization vs. liquid molar volume, for all ionic liquid species containing a 1-ethyl-3-methylimidazolium cation, as shown in Fig. 4. No simple correlation is obtained, as reported by Zaitsau et al. [31]. Two distinct areas and a certain area of transition of data accumulation are noticed, instead. The enthalpies of vaporization of 1-ethyl-3-methylimidazolium based ionic liquids vary by ~60 kJ mol^{-1}, depending on the chosen anion. Class 2 ionic liquids comprising fluorinated anions exhibit lower enthalpies of vaporization, varying with the degree of fluorination, symmetry, size and charge delocalization of the anion, with the enthalpies of vaporization descending in the order $[BF_4]^- \approx [PF_6]^- \approx [OTf]^- \approx [BTTI]^- > [NF]^- > [BETI]^- \approx [NTf_2]^- > [PO_2(C_2F_5)_2]^- > [FAP]^-$. Besides no reasonable correlations of enthalpies of vaporization with the normalized solvent polarity E_T^N and Kamlet–Taft parameters were found [31], similar sequences are reported from measurements of the Kamlet–Taft π^*-parameter of 1-butylimidazolium ionic liquids, describing dipolarity/polarizability effects, e.g., in *N*-methyl-3-dinitroaniline: [C_4C_1im][BF_4] > [C_4C_1im][PF_6] > [C_4C_1im][OTf] > [C_4C_1im][NTf_2] [65].

The enthalpies of vaporization for the bulk of remaining anions (forming class 1 ionic liquids) are distinctively higher and steadily increasing with its molar volume – in the case of alkylsulfate anions, with nearly the same increment as caused by an increase in the carbon numbers of the alkyl chain in the 1-alkyl-3-methylimidazolium bis(trifluoromethylsulfonyl) amide series, when starting from C3.

The enthalpies of vaporization increase in the following order: $[SCN]^- < [N(CN)_2]^- < [C_1SO_4]^- < [C_2SO_4]^- < [Tos]^- < [C_8SO_4]^-$. The enthalpy of vaporization of the class 1 ionic liquid [C_2C_1im][C_1SO_3] was found to be located somewhat lower from this trend, near the transition area formed by symmetrical and/or relatively small fluorinated anions, with no experimental data available yet for confirmation.

The inspection of the respective sigma profiles for ion pairs of each distinct area, as shown in Fig. 5, and corresponding sigma surfaces, as shown in Fig. 6, illustrates differences in the local polarization-charge densities, which ultimately define the differentiation in the interaction energies of the surfaces, and hence, the magnitude of the respective enthalpies of vaporization. The aromatic imidazolium ring with strongly delocalized positive charge, resulting in moderate polarization charge densities, is common to all depicted ion pairs. In [C_2C_1im][NTf_2], the anionic charge is delocalized by conjugation across several atoms, rendering the ion pair's surface weakly polar. In the highly symmetric hexafluorophosphate anion, the charge is delocalized over six fluorine ligands, resulting in a slightly more polar ion pair and a higher enthalpy of vaporization. In [C_2C_1im][C_2SO_4], considerable parts of the anionic surface portion exhibit an even higher polarity, hence, the enthalpy of vaporization increases even further.

3.5. Same anion, different cations

A similar discussion may be conducted for other ion pair combinations. The current availability on experimental data for other ionic liquid cations beyond alkylimidazolium can be described as limited, at best. Here, we examine combinations with the popular bis(trifluoromethylsulfonyl)amide as the chosen common anion, a sequence as presented in Fig. 7 is obtained.

In a first approximation, slightly more polar cations will result in higher enthalpies of vaporization, when compared with the less polar ones. When inspecting the results of ionic liquids with 1-n-butyl chains connected to the different cationic moieties, the order obtained is spanning a difference in enthalpy of vaporization of only ~20 kJ mol^{-1}: [C_4C_1morph][NTf_2] > [C_4py][NTf_2] ≈ [$C_4C_1C_1$im][NTf_2] > [C_4C_1pyrr][NTf_2] ≈ [$C_xC_1$pip][NTf_2] ≈ [C_4C_4im][NTf_2] > [C_4C_1im][NTf_2]. From previous measurements of the Kamlet–Taft π^*-parameter of 1-butylsubstituted ionic liquids with the bis(trifluoromethylsulfonyl)amide anion, the following sequence was reported, valid for all dyes used: [$C_4C_1C_1$im][NTf_2] > [C_4C_1im][NTf_2] > [C_4C_1pyrr][NTf_2] [65]. Another paper reports on π^* for partially different 1-butylsubstituted ionic liquids (in *N*,*N*-diethyl-4-dinitroaniline): [C_4C_1morph][NTf_2] > [C_4C_1im][NTf_2] > [C_4C_1pyrr][NTf_2] > [C_4py] [NTf_2] [66]. The currently available data only suggest a distinctively different dipolarity/polarizability for

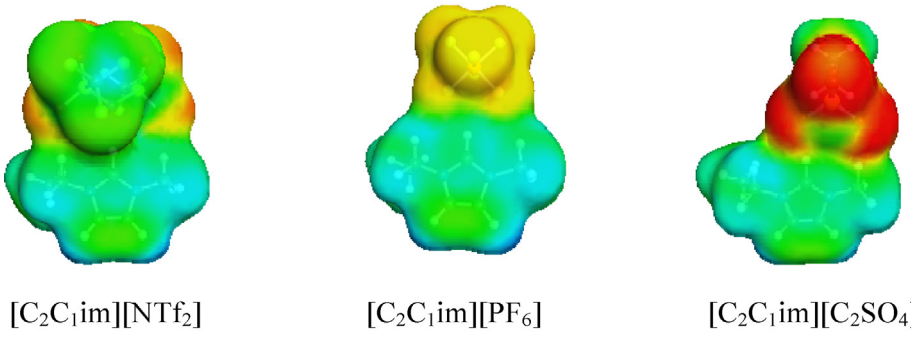

Fig. 6. Exemplary sigma surface plots of ion pairs, as obtained in this work. From left to the right: increasing polarity of the anionic component.

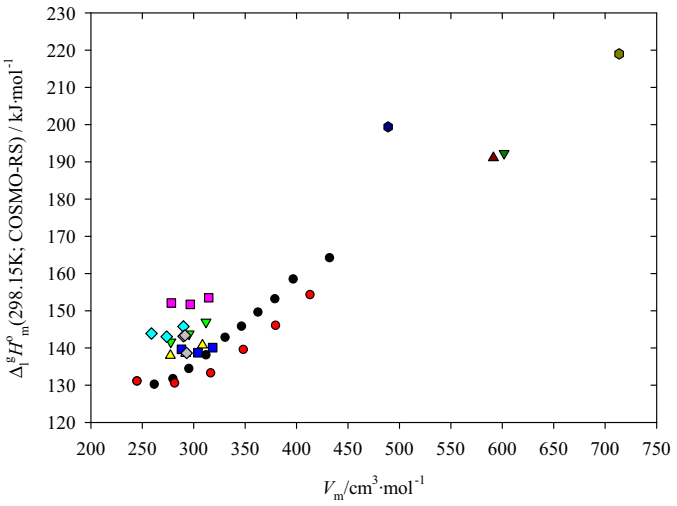

Fig. 7. Predicted enthalpies of vaporization of bis(trifluoromethylsulfonyl)amide based ionic liquids, at T = 298.15 K, as obtained with COSMO-RS, plotted against their respective liquid molar volume. ● : [$C_xC_1$im][NTf_2]; ● : [$C_xC_x$im][NTf_2]; ▼ : [$C_xC_1C_1$im][NTf_2]; ▲ : [$C_xC_1$pyrr][NTf_2]; ■ : [$C_xC_1$pip][NTf_2]; ■ : [$C_xC_1$morph][NTf_2]; ◆ : [$C_x$py][NTf_2]; ◆ : [$C_xC_y$py][NTf_2]; ▲ : [N_{8881}][NTf_2]; ▼ : [P_{8881}][NTf_2]; ⬢ : [P_{66614}][NTf_2]; ⬢ : [$C_3(C_1im)_2$][NTf_2]$_2$.

alkylated morpholinium salts, when compared with the other listed cations, whose polarity differentiation among them is more subtle.

4. Conclusions

Based on the availability of experimental data so far, it can be concluded that COSMO-RS is suitable to estimate enthalpies of vaporization of ionic liquids of varying composition with a sufficient degree of accuracy for practical purposes, especially against the background of current scatter in the available experimental data, thus contributing to the efforts of concisely tailoring ionic liquid properties. A more accurate approach for the refinement of enthalpy of vaporization data would include the application of an equilibrated set of conformers in the statistical COSMO-RS calculations, at the expense of a drastically increased computational load. Furthermore, in the recent COSMOtherm release (COSMOtherm Version C3.0 Release 13.01, as of December 2012 [67]), an improved hydrogen bond term (HB2012) at the BP-TZVPD-FINE level [68], based on a priori quantum chemistry considerations, was introduced, aiming at high quality predictions. In order to evaluate this methodology, further high-quality experimental enthalpies of vaporization data are of paramount importance.

Besides further improvements in the experimental methodology aiming at consistent data sets, more experimental data, covering a wider range of ionic liquids, are sought after. Ionic liquids of interest with respect to experimental enthalpies of vaporization determinations in the near future are alkylimidazolium with methylation in 2- and 5-position, dialkylpyrrolidinum, alkylpyridinium cations, ammonium and phosphonium cations, with a range of alkylation, combined with a variety of anions. Another route of research could include polyionic ionic liquids.

List of symbols

Notation

$\Delta_l^g H^o_m$	enthalpy of vaporization (kJ mol^{-1})
R	universal gas constant (J K^{-1} mol^{-1})
T	temperature (K)
V_m	liquid molar volume (cm^3 mol^{-1}) or (Å^3)
δ	Hildebrand solubility parameter (MPa$^{1/2}$)
c	cohesive pressure (MPa)
α_m	molar polarizability (Å^3)

Acknowledgments

Bernd Schröder acknowledges Fundação para a Ciência e a Tecnologia (FCT) and the European Social Fund (ESF) under the 3rd Community Support Framework (CSF) for the award of a post-doctoral grant (grant number SFRH/BPD/38637/2007) and the award of research project PTDC/AAC-AMB/121161/2010. On behalf of CICECO, the programme PEst-C/CTM/LA0011/2013 is acknowledged as well.

Appendix A. Supplementary data

Supplementary data associated with this article can be found, in the online version, at doi:10.1016/j.fluid.2014.02.026.

References

[1] J.M.S.S. Esperança, J.N. Canongia Lopes, M. Tariq, L.M.N.B.F. Santos, J.W. Magee, L.P.N. Rebelo, J. Chem. Eng. Data 55 (2010) 3–12, http://dx.doi.org/10.1021/je900458w.
[2] L.M.N.B.F. Santos, L.M.S.S. Lima, C.F.R.A.C. Lima, F.D. Magalhães, M.C. Torres, B. Schröder, M.A.V. Ribeiro da Silva, J. Chem. Thermodyn. 43 (2011) 834–843, http://dx.doi.org/10.1016/j.jct.2010.12.022.
[3] M.A.A. Rocha, C.F.R.A.C. Lima, L.R. Gomes, B. Schröder, J.A.P. Coutinho, I.M. Marrucho, J.M.S.S. Esperança, L.P.N. Rebelo, K. Shimizu, J.N. Canongia Lopes, L.M.N.B.F. Santos, J. Phys. Chem. B 115 (2011) 10919–10926, http://dx.doi.org/10.1021/jp2049316.
[4] S.P. Verevkin, D.H. Zaitsau, V.N. Emel'yanenko, A. Heintz, J. Phys. Chem. B 115 (2011) 12889–12895, http://dx.doi.org/10.1021/jp207397v.
[5] M.E.V. Valkenburg, R.L. Vaughn, M. Williams, J.S. Wilkes, Thermochim. Acta 425 (2005) 181–188, http://dx.doi.org/10.1016/j.tca.2004.11.013.
[6] B.Q. Wu, R.G. Reddy, R.D. Rogers, Novel ionic liquid thermal storage for solar thermal electric power systems, in: Proceedings of the International Solar Energy Conference, Washington, USA, 2001, p. 445.

[7] P. Wang, S.M. Zakeeruddin, I. Exnar, M. Grätzel, Chem. Commun. 297 (2002) 2–2973, http://dx.doi.org/10.1039/B209322G.
[8] T. Torimoto, K. Okazaki, T. Kiyama, K. Hirahara, N. Tanaka, S. Kuwabata, Appl. Phys. Lett. 89 (2006) 243117, http://dx.doi.org/10.1063/1.2404975.
[9] http://www.sigmaaldrich.com/analytical-chromatography/analytical-products.html?TablePage=101691909 (accessed 02.12.13).
[10] J.A.P. Coutinho, P.J. Carvalho, N.M.C. Oliveira, RSC Adv. 2 (2012) 7322–7346, http://dx.doi.org/10.1039/C2RA20141K.
[11] B. Kirchner, Top. Curr. Chem. 290 (2009) 213–262, http://dx.doi.org/10.1007/128_2008_36.
[12] S.H. Lee, S.B. Lee, Chem. Commun. (2005) 3469–3471, http://dx.doi.org/10.1039/B503740A.
[13] M.S. Kelkar, E.J. Maginn, J. Phys. Chem. B 111 (2007) 9424–9427.
[14] T. Köddermann, D. Paschek, R. Ludwig, ChemPhysChem 8 (2007) 2464–2470, http://dx.doi.org/10.1002/cphc.200700552.
[15] M.S. Kelkar, W. Shi, E.J. Maginn, Ind. Eng. Chem. Res. 47 (2008) 9115–9126, http://dx.doi.org/10.1021/ie800843u.
[16] M. Diedenhofen, A. Klamt, K. Marsh, A. Schäfer, Phys. Chem. Chem. Phys. 9 (2007) 4653–4656, http://dx.doi.org/10.1039/B706728C.
[17] M. Diedenhofen, A. Klamt, Fluid Phase Equilib. 294 (2010) 31–38, http://dx.doi.org/10.1016/j.fluid.2010.02.002.
[18] L.M.N.B.F. Santos, J.N. Canongia Lopes, J.A.P. Coutinho, J.M.S.S. Esperançą, L.R. Gomes, I.M. Marrucho, L.P.N. Rebelo, J. Am. Chem. Soc. 129 (2007) 284–285, http://dx.doi.org/10.1021/ja067427b.
[19] J.P. Leal, J.M.S.S. Esperançą, M.E. Minas da Piedade, J.N. Canongia Lopes, L.P.N. Rebelo, K.R. Seddon, J. Phys. Chem. A 111 (2007) 6176–6182, http://dx.doi.org/10.1021/jp073006k.
[20] D. Strasser, F. Goulay, M.S. Kelkar, E.J. Maginn, S.R. Leone, J. Phys. Chem. A 111 (2007) 3191–3195, http://dx.doi.org/10.1021/jp071323l.
[21] R.W. Berg, A. Riisager, R. Fehrmann, J. Phys. Chem. A 112 (2008) 8585–8592, http://dx.doi.org/10.1021/jp803597j.
[22] TURBOMOLE V6.2. A Development of University of Karlsruhe and Forschungszentrum Karlsruhe GmbH, 1989–2007, TURBOMOLE GmbH, 2010.
[23] L. Yang, S.I. Sandler, C. Peng, H. Liu, Y. Hu, Ind. Eng. Chem. Res. 49 (2010) 12596–12604, http://dx.doi.org/10.1021/ie1013647.
[24] F. Eckert, A. Klamt, AIChE J. 48 (2002) 369–385, http://dx.doi.org/10.1002/aic.690480220.
[25] F. Eckert, COSMOtherm User's Manual Version C2.1 Release 01.10, COSMOlogic GmbH & Co. KG, Leverkusen, 2009.
[26] F. Eckert, A. Klamt, COSMOtherm Version C2.1 Release 01.10, COSMOlogic GmbH & Co. KG, Leverkusen, 2009.
[27] U. Preiss, V.N. Emel'yanenko, S.P. Verevkin, D. Himmel, Y.U. Paulechka, I. Krossing, ChemPhysChem 11 (2010) 3425–3431, http://dx.doi.org/10.1002/cphc.201000614.
[28] S.P. Verevkin, D.H. Zaitsau, V.N. Emel'yanenko, A.V. Yermalayeu, C. Schick, H. Liu, E.J. Maginn, S. Bulut, I. Krossing, R. Kalb, J. Phys. Chem. B 117 (2013) 6473–6486, http://dx.doi.org/10.1021/jp311429r.
[29] H. Luo, G.A. Baker, S. Dai, J. Phys. Chem. B 112 (2008) 10077–10081, http://dx.doi.org/10.1021/jp805340f.
[30] D.H. Zaitsau, G.J. Kabo, A.A. Strechan, Y.U. Paulechka, A. Tschersich, S.P. Verevkin, A. Heintz, J. Phys. Chem. A 110 (2006) 7303–7306, http://dx.doi.org/10.1021/jp060896f.
[31] D.H. Zaitsau, K. Fumino, V.N. Emel'yanenko, A.V. Yermalayeu, R. Ludwig, S.P. Verevkin, ChemPhysChem 13 (2012) 1868–1876, http://dx.doi.org/10.1002/cphc.201100879.
[32] V.N. Emel'yanenko, S.P. Verevkin, A. Heintz, J. Am. Chem. Soc. 129 (2007) 3930–3937, http://dx.doi.org/10.1021/ja0679174.
[33] J.P. Armstrong, C. Hurst, R.G. Jones, P. Licence, K.R.J. Lovelock, C.J. Satterley, I.J. Villar-Garcia, Phys. Chem. Chem. Phys. 9 (2007) 982–990, http://dx.doi.org/10.1039/B615137J.
[34] F. Heym, B.J.M. Etzold, C. Kern, A. Jess, Green Chem. 13 (2011) 1453–1466, http://dx.doi.org/10.1039/C0GC00876A.
[35] D.H. Zaitsau, S.P. Verevkin, V.N. Emel'yanenko, A. Heintz, ChemPhysChem 12 (2011) 3609–3613, http://dx.doi.org/10.1002/cphc.201100618.
[36] K. Swiderski, A. McLean, C.M. Gordon, D.H. Vaughan, Chem. Commun. 217 (2004) 8–2179, http://dx.doi.org/10.1039/B408334B.
[37] Y.U. Paulechka, D.H. Zaitsau, G.J. Kabo, A.A. Strechan, Thermochim. Acta 439 (2005) 158–160, http://dx.doi.org/10.1016/j.tca.2005.08.035.
[38] F. Heym, B.J.M. Etzold, C. Kern, A. Jess, Phys. Chem. Chem. Phys. 12 (2010) 12089–12100, http://dx.doi.org/10.1039/C0CP00097C.
[39] S.D. Chambreau, G.L. Vaghjiani, A. To, C. Koh, D. Strasser, O. Kostko, S.R. Leone, J. Phys. Chem. B 114 (2010) 1361–1367, http://dx.doi.org/10.1021/jp909423m.
[40] A. Deyko, K.R.J. Lovelock, J.-A. Corfield, A.W. Taylor, P.N. Gooden, I.J. Villar-Garcia, P. Licence, R.G. Jones, V.G. Krasovskiy, E.A. Chernikova, L.M. Kustov, Phys. Chem. Chem. Phys. 11 (2009) 8544–8555, http://dx.doi.org/10.1039/B908209C.
[41] A. Deyko, S.G. Hessey, P. Licence, E.A. Chernikova, V.G. Krasovskiy, L.M. Kustov, R.G. Jones, Phys. Chem. Chem. Phys. 14 (2012) 3181–3193, http://dx.doi.org/10.1039/C2CP23705A.
[42] S.P. Verevkin, V.N. Emel'yanenko, D.H. Zaitsau, A. Heintz, C.D. Muzny, M. Frenkel, Phys. Chem. Chem. Phys. 12 (2010) 14994–15000, http://dx.doi.org/10.1039/C0CP00747A.
[43] V.N. Emel'yanenko, S.P. Verevkin, A. Heintz, J.-A. Corfield, A. Deyko, K.R.J. Lovelock, P. Licence, R.G. Jones, J. Phys. Chem. B 112 (2008) 11734–11742, http://dx.doi.org/10.1021/jp803238t.
[44] K.R.J. Lovelock, A. Deyko, J.-A. Corfield, P.N. Gooden, P. Licence, R.G. Jones, ChemPhysChem 10 (2009) 337–340, http://dx.doi.org/10.1002/cphc.200800690.
[45] J. Vitorino, J.P. Leal, P. Licence, K.R.J. Lovelock, P.N. Gooden, M.E. Minas da Piedade, K. Shimizu, L.P.N. Rebelo, J.N. Canongia Lopes, ChemPhysChem 11 (2010) 3673–3677, http://dx.doi.org/10.1002/cphc.201000723.
[46] J. Palomar, V.R. Ferro, J.S. Torrecilla, F. Rodríguez, Ind. Eng. Chem. Res. 46 (2007) 6041–6048, http://dx.doi.org/10.1021/ie070445x.
[47] M.L.S. Batista, C.M.S.S. Neves, P.J. Carvalho, R. Gani, J.A.P. Coutinho, J. Phys. Chem. B 115 (2011) 12879–12888, http://dx.doi.org/10.1021/jp207369g.
[48] C. Reichardt, Solvents and Solvent Effects in Organic Chemistry, Wiley-VCH, Weinheim, 2003, http://dx.doi.org/10.1002/3527601791.
[49] A.F.M. Barton, Handbook of Solubility Parameters and other Cohesion Parameters, CRC Press, Boca Raton, FL, 1983.
[50] A. Triolo, O. Russina, H.-J. Bleif, E. Di Cola, J. Phys. Chem. B 111 (2007) 4641–4644, http://dx.doi.org/10.1021/jp067705t.
[51] O. Russina, A. Triolo, L. Gontrani, R. Caminiti, D. Xiao, L.G. Hines Jr., R.A. Bartsch, E.L. Quitevis, N. Plechkova, K.R. Seddon, J. Phys. Condens. Matter 21 (2009) 424121, http://dx.doi.org/10.1088/0953-8984/21/42/424121.
[52] A. Triolo, O. Russina, B. Fazio, G.B. Appetecchi, M. Carewska, S. Passerini, J. Chem. Phys. 130 (2009) 164521–164526, http://dx.doi.org/10.1063/1.3119977.
[53] M.A.A. Rocha, M. Bastos, J.A.P. Coutinho, L.M.N.B.F. Santos, J. Chem. Thermodyn. 53 (2012) 140–143, http://dx.doi.org/10.1016/j.jct.2012.04.025.
[54] J.N.A. Canongia Lopes, A.A.H. Pádua, J. Phys. Chem. B 110 (2006) 3330–3335, http://dx.doi.org/10.1021/jp056006y.
[55] K. Shimizu, A.A.H. Pádua, J.N. Canongia Lopes, J. Phys. Chem. B 114 (2010) 15635–15641, http://dx.doi.org/10.1021/jp108420x.
[56] K. Shimizu, M.F. Costa Gomes, A.A.H. Pádua, L.P.N. Rebelo, J.N. Canongia Lopes, J. Mol. Struct. THEOCHEM 946 (2010) 70–76, http://dx.doi.org/10.1016/j.theochem.2009.11.034.
[57] Y. Zhang, E.J. Maginn, Phys. Chem. Chem. Phys. 14 (2012) 12157–12164, http://dx.doi.org/10.1039/C2CP41964E.
[58] K. Noack, P.S. Schulz, N. Paape, J. Kiefer, P. Wasserscheid, A. Leipertz, Phys. Chem. Chem. Phys. 12 (2010) 14153–14161, http://dx.doi.org/10.1039/C0CP00486C.
[59] K. Fumino, A. Wulf, R. Ludwig, Phys. Chem. Chem. Phys. 11 (2009) 8790–8794, http://dx.doi.org/10.1039/B905634C.
[60] C. Roth, T. Peppel, K. Fumino, M. Köckerling, R. Ludwig, Angew. Chem. Int. Ed. 49 (2010) 10221–10224, http://dx.doi.org/10.1002/anie.201004955.
[61] K. Shimizu, M. Tariq, M.F. Costa Gomes, L.P.N. Rebelo, J.N. Canongia Lopes, J. Phys. Chem. B 114 (2010) 5831–5834, http://dx.doi.org/10.1021/jp101910c.
[62] K. Bica, M. Deetlefs, C. Schröder, K.R. Seddon, Phys. Chem. Chem. Phys. 15 (2013) 2703–2711, http://dx.doi.org/10.1039/C3CP43867H.
[63] S. Seki, S. Tsuzuki, K. Hayamizu, Y. Umebayashi, N. Serizawa, K. Takei, H. Miyashiro, J. Chem. Eng. Data 57 (2012) 2211–2216, http://dx.doi.org/10.1021/je201289w.
[64] J.L. Anderson, R. Ding, A. Ellern, D.W. Armstrong, J. Am. Chem. Soc. 127 (2005) 593–604, http://dx.doi.org/10.1021/ja046521u.
[65] M.A. Ab Rani, A. Brant, L. Crowhurst, A. Dolan, M. Lui, N.H. Hassan, J.P. Hallett, P.A. Hunt, H. Niedermeyer, J.M. Perez-Arlandis, M. Schrems, T. Welton, R. Wilding, Phys. Chem. Chem. Phys. 13 (2011) 16831–16840, http://dx.doi.org/10.1039/C1CP21262A.
[66] C. Chiappe, C.S. Pomelli, S. Rajamani, J. Phys. Chem. B 115 (2011) 9653–9661, http://dx.doi.org/10.1021/jp2045788.
[67] F. Eckert, A. Klamt, COSMOtherm Version C3.01 Release 13.01, COSMOlogic GmbH & Co. KG, Leverkusen, Germany, 2013.
[68] F. Eckert, COSMOtherm User's Manual Version C3.0 Release 13.01, COSMOlogic GmbH & Co. KG, Leverkusen, 2013.